

**The synthesis of tetraarylethylene-based conjugated polymers for the application  
of fluorescence sensing towards nitroaromatics**

Rentuya Wu<sup>a, #</sup>, Xiaosong Sun<sup>a, #</sup>, Wenyue Dong<sup>a, b, \*</sup>, Yanwei Li<sup>a</sup>, Qian Duan<sup>a, c, \*</sup>, Teng Fei<sup>d</sup>

<sup>a</sup> School of Materials Science and Engineering, Changchun University of Science and Technology, Changchun, 130022, PR China

<sup>b</sup> Chongqing Research Institute, Changchun University of Science and Technology, Chongqing, 401135, PR China

<sup>c</sup> Engineering Research Center for Optoelectronic Functional Materials, Ministry of Education, Changchun, 130022, PR China

<sup>d</sup> State Key Laboratory of Integrated Optoelectronics, College of Electronic Science and Engineering, Jilin University, Changchun, 130012, PR China

\*Corresponding author:

dongwenyue@cust.edu.cn (W. Dong)

duanqian88@hotmail.com (Q. Duan)

#These authors contributed equally to this manuscript.

## Content

Reagents and equipment

Scheme S1 Synthetic routes to M1, M2 and M3.

Figure S1 (a) FT-IR spectra of thioxanthene-9-one and M1; (b)  $^1\text{H}$  NMR spectrum of M1.

Figure S2 (a) FT-IR spectra of 9,9-dihexyl-2,7-dibromofluorene and M2; (b)  $^1\text{H}$  NMR spectrum of M2.

Figure S3 (a) FT-IR spectra of 3,6-dibromo-9-heptyl-9H-carbazole and M3; (b)  $^1\text{H}$  NMR spectrum of M3.

Figure S4  $^{13}\text{C}$  NMR spectrum of (a) PT-F and (b) PT-Cz in  $\text{C}_2\text{D}_2\text{Cl}_4$ .

Figure S5 Linear fitting of fluorescence intensities of (a) PT-F and (b) PT-Cz versus TNP concentration.

Table S1 Sensing parameters of PT-F and PT-Cz for TNP.

Figure S6 PL spectra of (a) PT-F and (b) PT-Cz solutions upon pure water (same volume of TNP solution) addition.

Figure S7 Fluorescence quenching spectra of (a) PT-F and (c) PT-Cz upon TNB addition; SV plots of relative fluorescence intensities  $I_0/I-1$  of (b) PT-F and (d) PT-Cz versus TNB concentration.

Figure S8 Linear fitting of fluorescence intensities of (a) PT-F and (b) PT-Cz versus TNB concentration.

Figure S9 Fluorescence quenching spectra of (a) PT-F and (c) PT-Cz upon DNP addition; SV plots of relative fluorescence intensities  $I_0/I-1$  of (b) PT-F and (d) PT-Cz versus DNP concentration.

Figure S10 Linear fitting of fluorescence intensities of (a) PT-F and (b) PT-Cz versus DNP concentration.

Figure S11 Fluorescence quenching spectra of (a) PT-F and (c) PT-Cz upon 4-NP addition; SV plots of relative fluorescence intensities  $I_0/I-1$  of (b) PT-F and (d) PT-Cz versus 4-NP concentration.

Figure S12 Linear fitting of fluorescence intensities of (a) PT-F and (b) PT-Cz versus 4-NP

concentration.

Table S2 Sensing parameters of PT-F and PT-Cz for various nitroaromatics.

Figure S13 Linear fitting of relative fluorescence intensities of (a) PT-F and (c) PT-Cz versus TNP concentration (mg/L); (c) calibration curve of HPLC analysis for TNP.

Table S3 t-test table.

Figure S14 Cyclic voltammograms of (a) PT-F and (b) PT-Cz in acetonitrile (electrolyte: 0.1 M TBAPF<sub>6</sub>).

Figure S15 UV-Vis absorption spectra of various nitroaromatics.

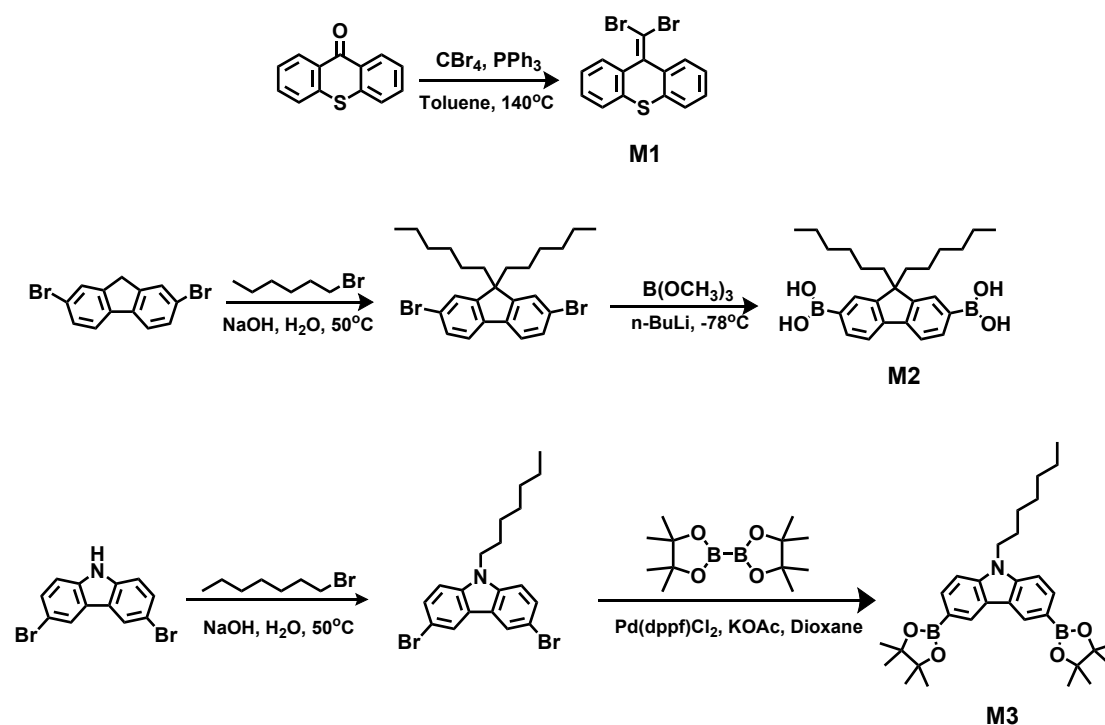
Figure S16 Time resolved fluorescence spectra of (a) PT-F and (c) PT-Cz before and after the addition of TNP.

## Reagents and equipment

Thioxanthen-9-one, tetrabutylammonium bromide, 2,7-dibromofluorene, 1-bromohexane, 3,6-dibromocarbazole, 1-bromoheptane, n-butyllithium (n-BuLi), tetrahydrofuran (THF), 1,4-dioxane, dichloromethane, petroleum, triphenylphosphine, [1,1'-Bis(diphenylphosphino)ferrocene]dichloropalladium(II) potassium carbonate, magnesium sulfate, tetrakis(triphenylphosphine)palladium, calcium hydroxide, sodium hydroxide and ammonium chloride were purchased from Energy Chemical. Bis(pinacolato)diboron, potassium acetate, carbon tetrabromide and toluene were purchased from Aladdin.

The Fourier transform infrared (FT-IR) spectra were obtained on a Frontier FT-IR spectrometer.  $^1\text{H}$  and  $^{13}\text{C}$  NMR spectra were measured on Bruker AV 500 spectrometers at 298 K and tetramethylsilane as standard. A Waters 510 gel permeation chromatograph was used to test the GPC. UV-Visible (UV-Vis) spectra were tested by UV-1240 UV-Vis spectrophotometer of SHIMADZU. Fluorescence spectra were measured on the fluorescence spectrometer LS-55 of PerkinElmer. The cyclic voltammetry (CV) curves were tested by 100 B/W of BAS electrochemical workstation. The initial oxidation potential  $E_{OX}^{onset}$  was determined according to the intersection of two tangents drawn at the rising current and background current in the CV curve. Time-resolved fluorescence spectra were measured on Flou Time 300 automatic fluorescence lifetime spectrometer of Wuhan Donglong Technology Co., Ltd, and the fluorescence lifetimes were calculated according to the formula 
$$\tau = \frac{A_1\tau_1^2 + A_2\tau_2^2}{A_1\tau_1 + A_2\tau_2}$$
. The high-performance liquid chromatography (HPLC) was obtained on a Shimadzu Essentia LC-16 chromatography. For HPLC analysis, the C<sub>18</sub> column

(250×4.6 mm<sup>2</sup> i.d., 5 μm, Kromasil) was used as a stationary phase and 357 nm was chosen as detection wavelength with 3 nm slit width. Herein, methanol/water (70/30, V/V) was used as a mobile phase with 0.500 mL/min flow rate and isocratic elution was applied at room temperature. The column temperature was set at 40 °C and the sample injection volume was 10 μL.



Scheme S1 Synthetic routes to M1, M2 and M3.

### 9-(Dibromomethylene)-9H-thioxanthen-9-one (M1)

The Corey-Fushs reaction was used to prepare monomer M1. Thioxanthen-9-one (1.96 g, 10.0 mmol), carbon tetrabromide (6.63 g, 20.0 mmol) and triphenylphosphine (8.77 g, 40.0 mmol) were added to 50 mL anhydrous toluene. After degassing by freeze-thaw for three times, the reaction was stirred at 140 °C for 72 h. The filtrate was filtered and washed with toluene, and then column chromatographed with petroleum ether to obtain a light yellow powder (yield 81%). FT-IR (KBr pellet):

$\nu=1583, 1430, 1274, 1039, 790, 621 \text{ cm}^{-1}$ .  $^1\text{H NMR}$  (500 MHz,  $\text{CDCl}_3$ , ppm):  $\delta=7.81$  (d,  $J=7.3 \text{ Hz}$ , 2H), 7.53 (d,  $J=7.4 \text{ Hz}$ , 2H), 7.33 (t,  $J=7.4 \text{ Hz}$ , 4H).

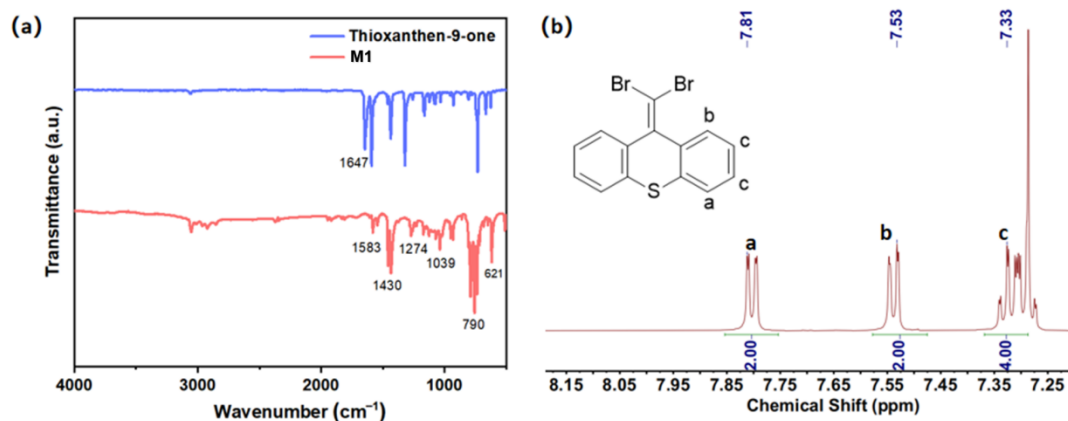


Figure S1 (a) FT-IR spectra of thioxanthen-9-one and M1; (b)  $^1\text{H NMR}$  spectrum of M1.

### **(9,9-Dihexyl-9H-fluorene-2,7-diyl)diboronic acid (M2)**

The precursor 2,7-dibromo-9,9-dihexyl-9H-fluorene was synthesized as following. 2,7-Dibromofluorene (3.24 g, 10.0 mmol) and tetrabutylammonium bromide (0.10 g, 0.03 mmol) were added to a mixture of 20 mL of 1-bromohexane and 20 mL of sodium hydroxide water solution (50%). After degassing for three times, the reaction was stirred at 50 °C for 24 h. The mixture was extracted with dichloromethane, and the organic phase was dried over  $\text{MgSO}_4$ . After filtration and concentration, the crude product was column chromatographed with dichloromethane/petroleum ether (3/7, V/V) to obtain white powder (yield 72%). FT-IR (KBr pellet):  $\nu=2932, 2853, 1722, 1592, 1443, 1114, 772, 681 \text{ cm}^{-1}$ .

The monomer M2 was synthesized via Miyaura reaction. 2,7-Dibromo-9,9-dihexyl-9H-fluorene (2.59 g, 5.0 mmol) was dissolved in 50 mL anhydrous THF, and the mixture was degassed for 3 times and cooled to  $-78 \text{ }^\circ\text{C}$ . Under nitrogen, n-BuLi (0.80 g, 12.5 mmol) was added to the mixture drop by drop, and trimethyl borate (1.56 g, 15.0 mmol) was slowly added while the temperature was kept at  $-78 \text{ }^\circ\text{C}$  for 1.5 h.

After stirring for 1.5 h and gradually heating up to room temperature for 24 h, the reaction was quenched with ammonium chloride solution, and extracted with dichloromethane. After filtration and concentration, the crude product was column chromatographed with dichloromethane/petroleum ether (2/5, V/V) to obtain white powder (yield 50%). FT-IR (KBr pellet):  $\nu=3433, 2925, 2855, 1612, 1348, 1142, 751$   $\text{cm}^{-1}$ .  $^1\text{H NMR}$  (500 MHz,  $\text{CDCl}_3$ ):  $\delta$  (ppm) 7.82 (d,  $J=7.6$  Hz, 2H), 7.74 (d,  $J=7.6$  Hz, 4H), 2.03–1.91 (m, 4H), 1.10–0.78 (m, 16H), 0.77 (t,  $J=7.2$  Hz, 6H).

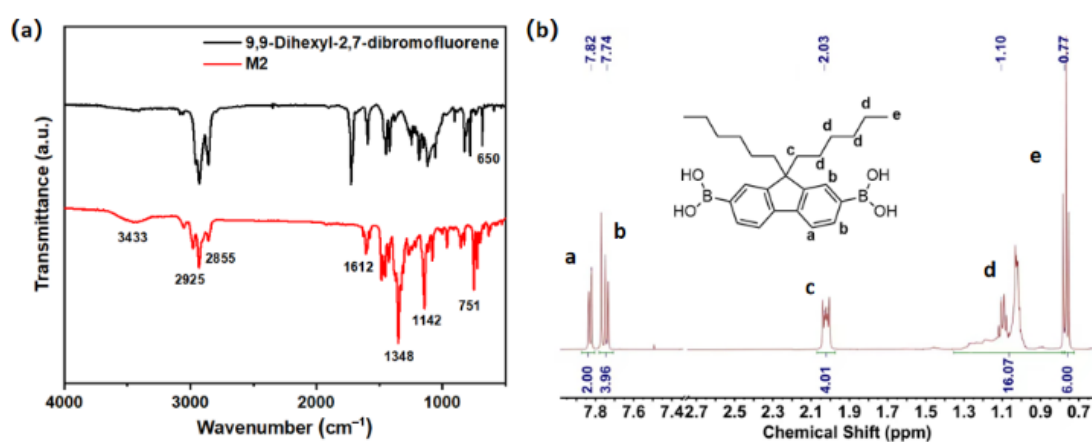


Figure S2 (a) FT-IR spectra of 9,9-dihexyl-2,7-dibromofluorene and M2; (b)  $^1\text{H NMR}$  spectrum of M2.

### 9-Heptyl-3,6-bis(4,4,5,5-tetramethyl-1,3,2-dioxaborolan-2-yl)-9H-carbazole (M3)

The precursor 3,6-dibromo-9-heptyl-9H-carbazole was synthesized as following. 3,6-Dibromocarbazole (3.25 g, 10.0 mmol) and tetrabutylammonium bromide (0.10 g, 0.03 mmol) were added to a mixture of 20 mL 1-bromoheptane and 20 mL sodium hydroxide aqueous solution (50%). The mixture was degassed three times, and stirred at 50 °C for 24 h. Then the reaction was extracted with dichloromethane, and purified with dichloromethane/petroleum ether (1/3, V/V) (yield 69%). FT-IR (KBr pellet):  $\nu=2925, 2857, 1472, 1380, 1248, 1018, 800, 646$   $\text{cm}^{-1}$ .

The monomer M3 was prepared by Miyaura reaction. 3,6-Dibromo-9-heptyl-9H-carbazole (2.12 g, 5.0 mmol), bis(pinacolato)diboron (3.17 g, 12.5 mmol) and

potassium acetate (1.47 g, 15.0 mmol) were added to 50 mL of anhydrous 1,4-dioxane. Under nitrogen, Pd(dppf)<sub>2</sub>Cl<sub>2</sub> (0.37 mg, 0.5 mmol) was added and stirred at 90 °C for 12 h, then the filtrate was extracted with ethyl acetate, collected and dried. White powder was obtained by column chromatography with ethyl acetate/petroleum ether (1/10, V/V) (yield 48%). FT-IR (KBr pellet):  $\nu=2925, 2857, 1348, 1129, 852, 680$  cm<sup>-1</sup>. <sup>1</sup>H NMR (500 MHz, CDCl<sub>3</sub>, ppm):  $\delta$  8.69 (s, 2H), 7.92 (d, J=8.4 Hz, 2H), 7.42 (d, J=8.4 Hz, 2H), 4.34 (t, J=7.2 Hz, 2H), 1.88 (t, J=7.5 Hz, 2H), 1.41 (s, 8H), 1.29 (s, 24H), 0.87 (t, J=7.0 Hz, 3H).

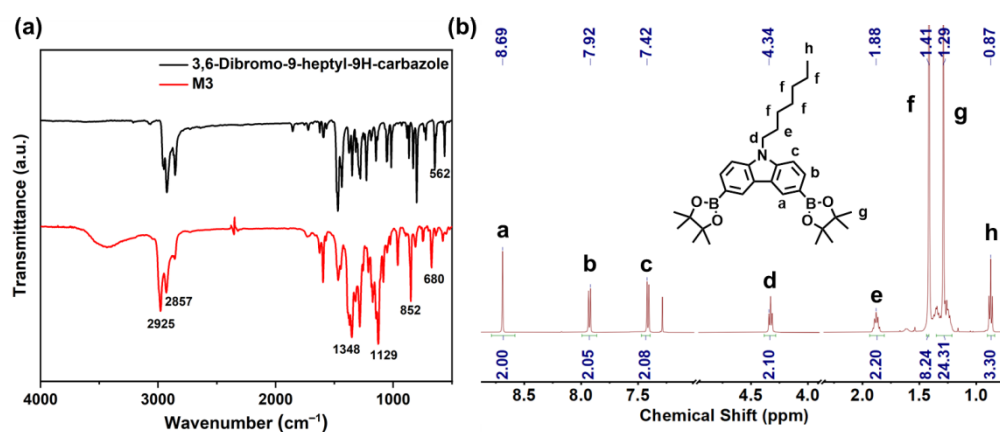


Figure S3 (a) FT-IR spectra of 3,6-dibromo-9-heptyl-9H-carbazole and M3; (b) <sup>1</sup>H NMR spectrum of M3.

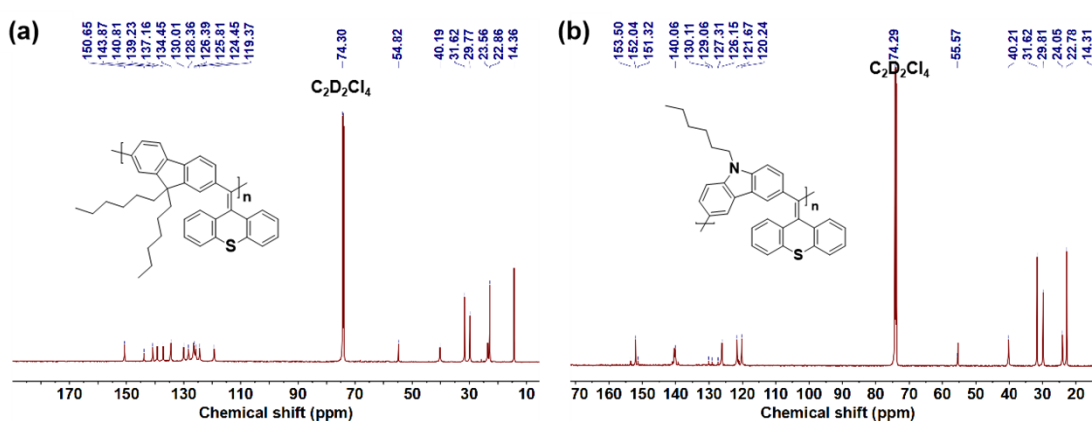


Figure S4 <sup>13</sup>C NMR spectrum of (a) PT-F and (b) PT-Cz in C<sub>2</sub>D<sub>2</sub>Cl<sub>4</sub>.



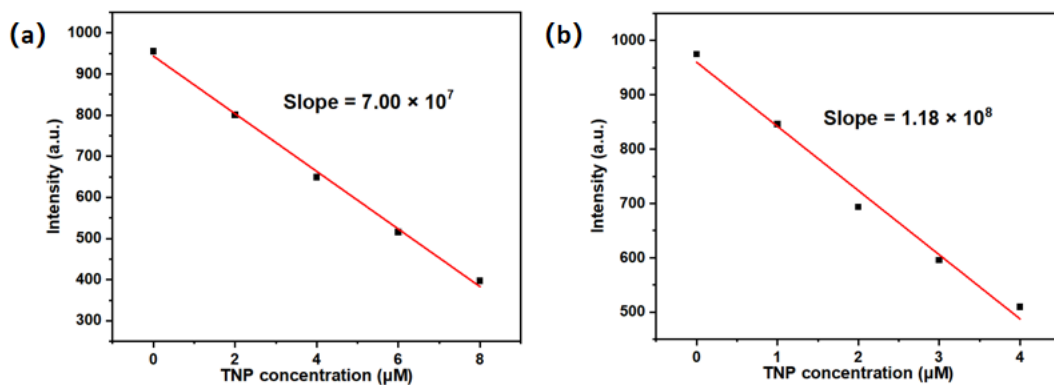


Figure S5 Linear fitting of fluorescence intensities of (a) PT-F and (b) PT-Cz versus TNP concentration.

Table S1 Sensing parameters of PT-F and PT-Cz for TNP.

| Polymer | $\sigma$ | Slope                             | LOD                | LOQ                |
|---------|----------|-----------------------------------|--------------------|--------------------|
| PT-F    | 2.80     | $7.00 \times 10^7 \text{ M}^{-1}$ | $0.12 \mu\text{M}$ | $0.40 \mu\text{M}$ |
| PT-Cz   | 2.68     | $1.18 \times 10^8 \text{ M}^{-1}$ | $0.07 \mu\text{M}$ | $0.23 \mu\text{M}$ |

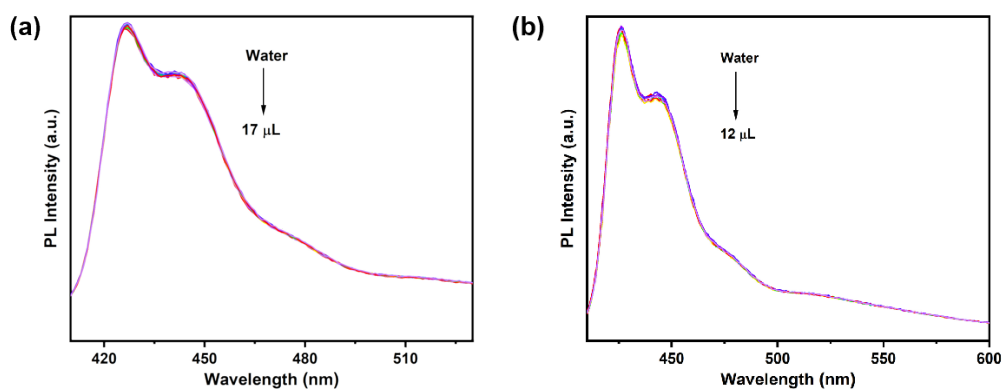


Figure S6 PL spectra of the (a) PT-F and (b) T-Cz solutions upon pure water (same volume of TNP solution) addition.

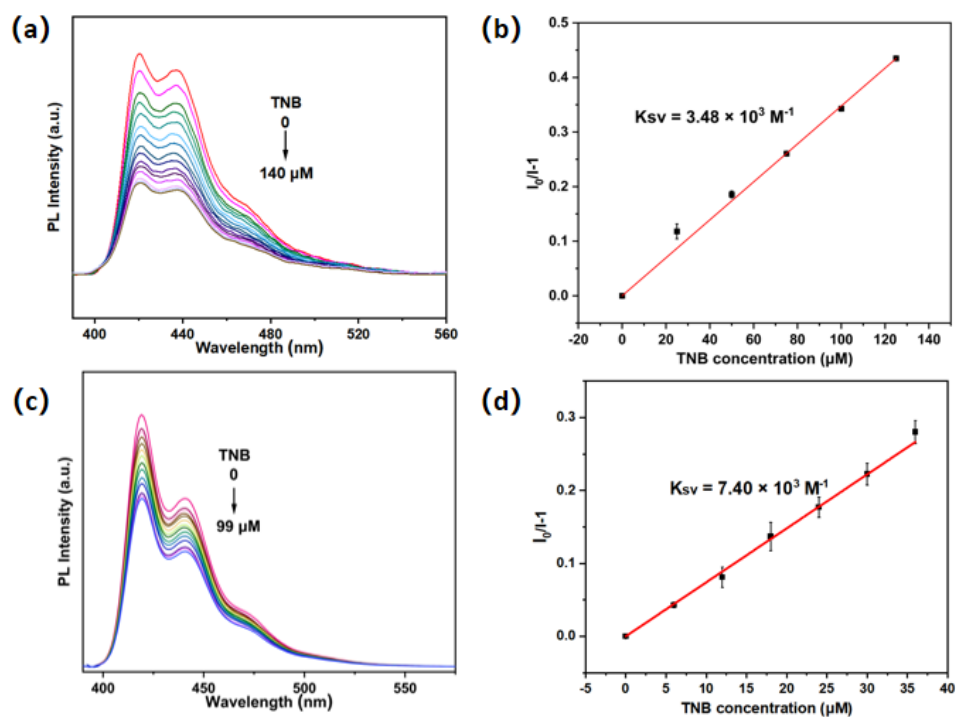


Figure S7 Fluorescence quenching spectra of (a) PT-F and (c) PT-Cz upon TNB addition; SV plots of relative fluorescence intensities  $I_0/I-1$  of (b) PT-F and (d) PT-Cz versus TNB concentration.

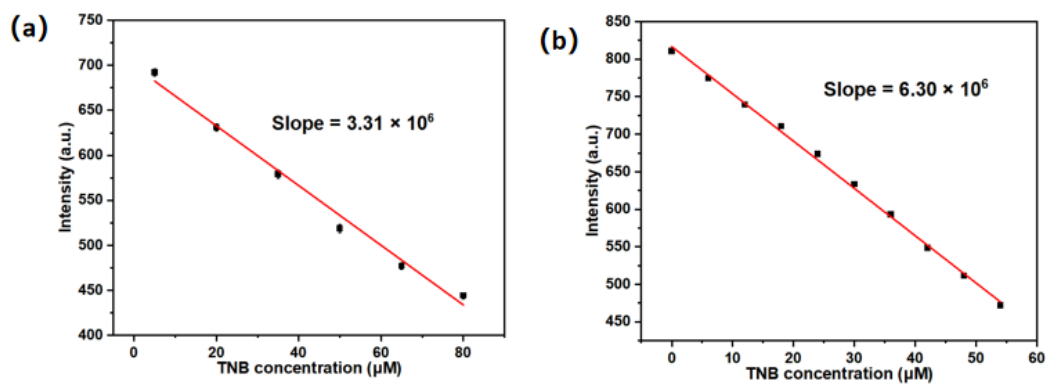


Figure S8 Linear fitting of fluorescence intensities of (a) PT-F and (b) PT-Cz versus TNB concentration.

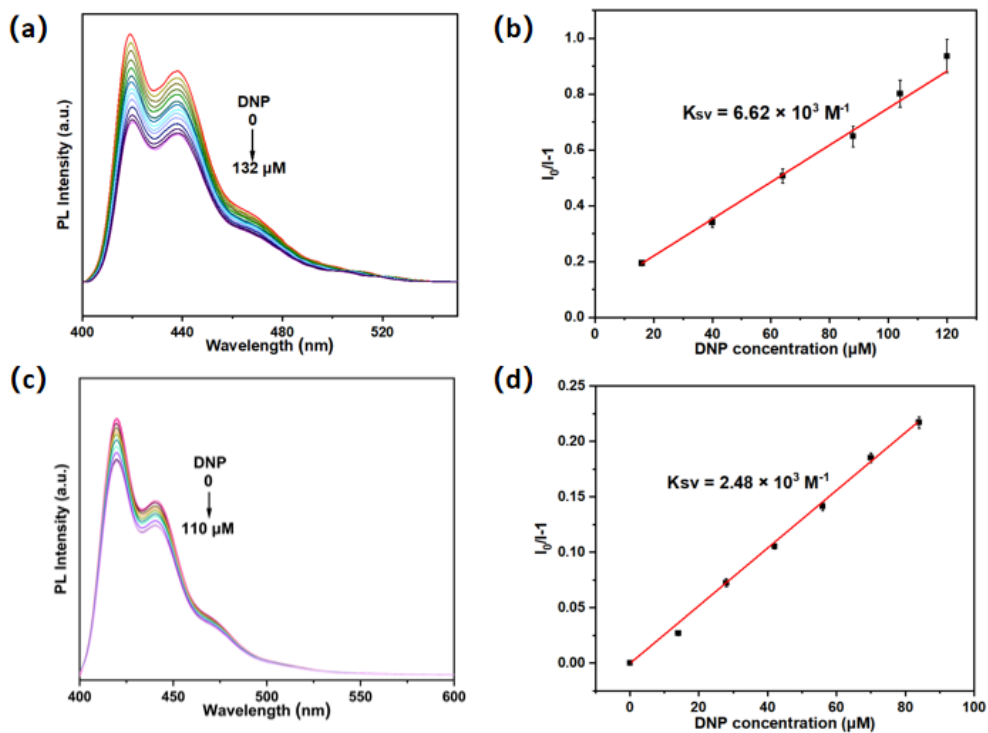


Figure S9 Fluorescence quenching spectra of (a) PT-F and (c) PT-Cz upon DNP addition; SV plots of relative fluorescence intensities  $I_0/I-1$  of (b) PT-F and (d) PT-Cz versus DNP concentration.

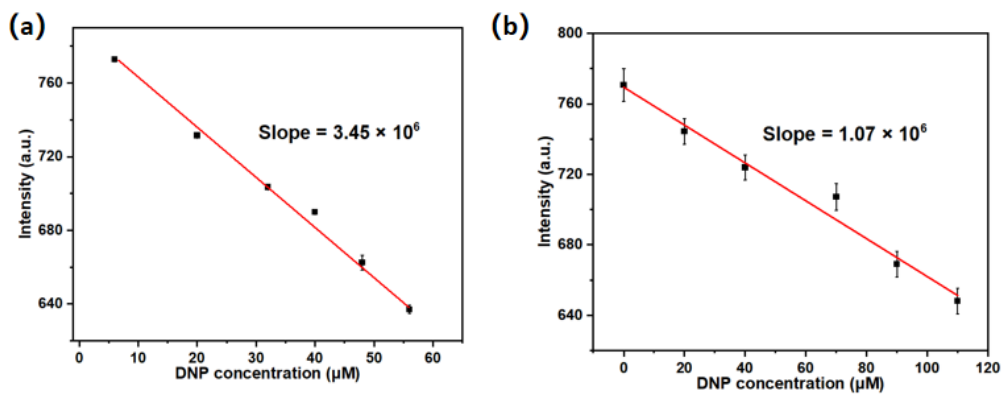


Figure S10 Linear fitting of fluorescence intensities of (a) PT-F and (b) PT-Cz versus DNP concentration.

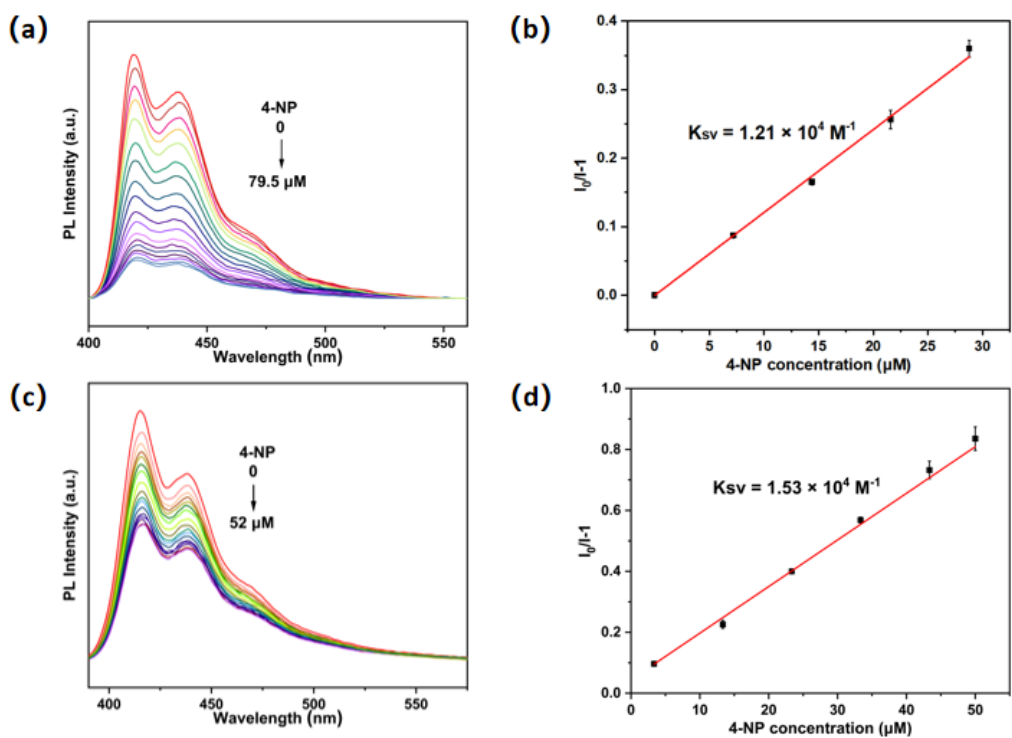


Figure S11 Fluorescence quenching spectra of (a) PT-F and (c) PT-Cz upon 4-NP addition; SV plots of relative fluorescence intensities  $I_0/I-1$  of (b) PT-F and (d) PT-Cz versus 4-NP concentration.

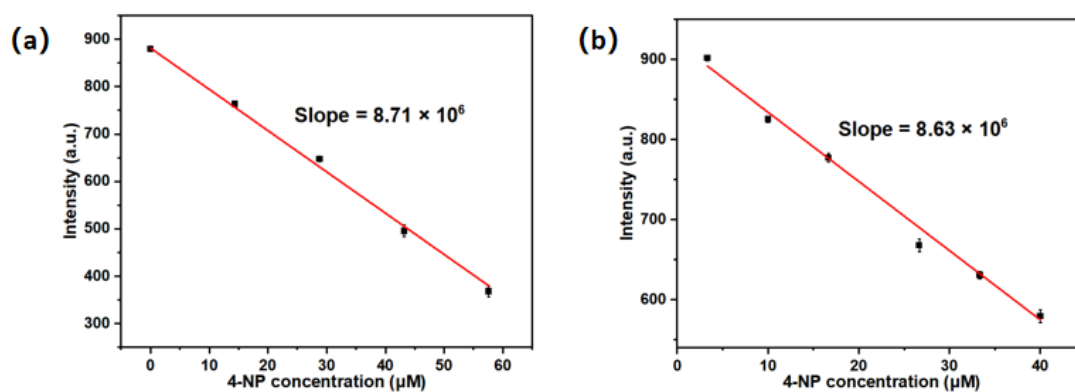


Figure S12 Linear fitting of fluorescence intensities of (a) PT-F and (b) PT-Cz versus 4-NP concentration.

Table S2 Sensing parameters of PT-F and PT-Cz for various nitroaromatics.

| Polymer | nitroaromatics | $K_{SV}$ ( $M^{-1}$ ) | LOD ( $\mu M$ ) | LOQ ( $\mu M$ ) |
|---------|----------------|-----------------------|-----------------|-----------------|
| PT-F    | TNP            | $1.20 \times 10^5$    | 0.12            | 0.40            |
|         | TNB            | $3.48 \times 10^3$    | 2.54            | 8.46            |
|         | DNP            | $6.62 \times 10^3$    | 2.43            | 8.12            |
|         | 4-NP           | $1.21 \times 10^4$    | 0.96            | 3.21            |
| PT-Cz   | TNP            | $2.04 \times 10^5$    | 0.07            | 0.23            |
|         | TNB            | $7.40 \times 10^3$    | 1.27            | 4.25            |
|         | DNP            | $2.48 \times 10^3$    | 3.24            | 10.81           |
|         | 4-NP           | $1.53 \times 10^4$    | 0.93            | 3.11            |

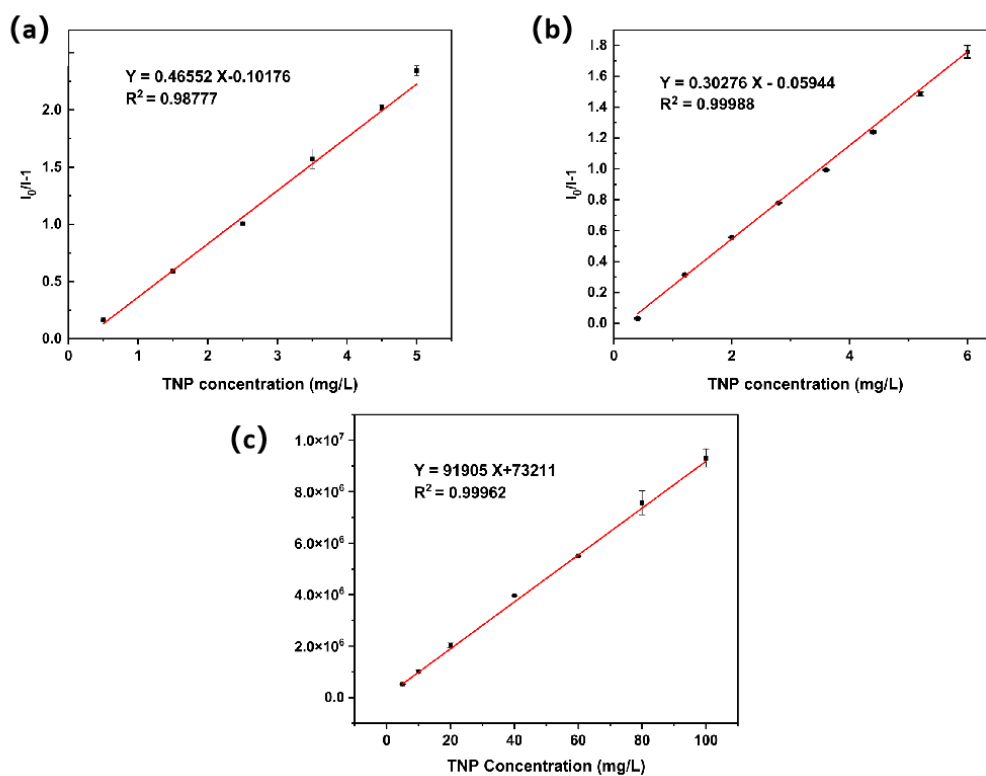


Figure S13 Linear fitting of relative fluorescence intensities of (a) PT-F and (c) PT-Cz versus TNP concentration (mg/L); (c) calibration curve of HPLC analysis for TNP.

Table S3 t-test table.

| Polymer | Water sample  | S    | $X_R$ | $\bar{X}$ | $t_{exp} = \frac{ X_R - \bar{X} }{S/\sqrt{n}}$ | $t_{ref}$ | Result     |
|---------|---------------|------|-------|-----------|--|-----------|------------|
|         | Lake water    | 0.46 | 5.00  | 5.39      | 1.47   | 4.30      | Acceptable |
| PT-F    | Tap water     | 0.31 | 5.00  | 4.66      | 1.90   | 4.30      | Acceptable |
|         | Mineral water | 0.21 | 5.00  | 5.14      | 1.16   | 4.30      | Acceptable |
|         | Lake water    | 0.29 | 5.00  | 5.31      | 1.86   | 4.30      | Acceptable |
| PT-Cz   | Tap water     | 0.16 | 5.00  | 4.70      | 3.26   | 4.30      | Acceptable |
|         | Mineral water | 0.13 | 5.00  | 5.11      | 1.47   | 4.30      | Acceptable |

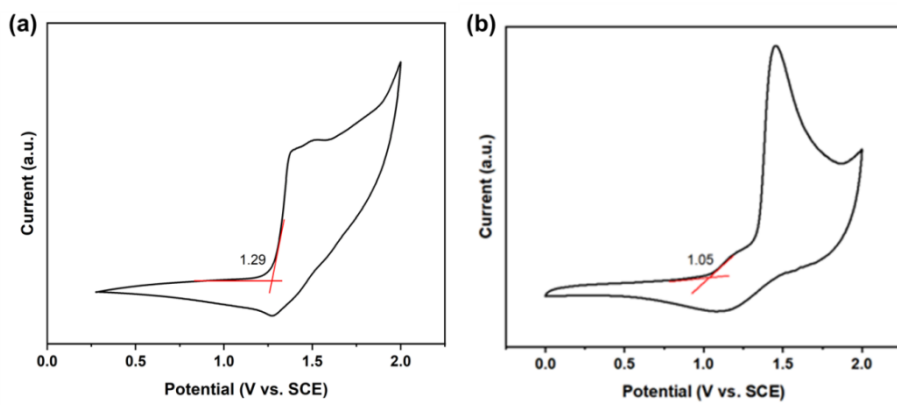


Figure S14 Cyclic voltammograms of (a) PT-F and (b) PT-Cz in acetonitrile (electrolyte: 0.1 M TBAPF<sub>6</sub>).

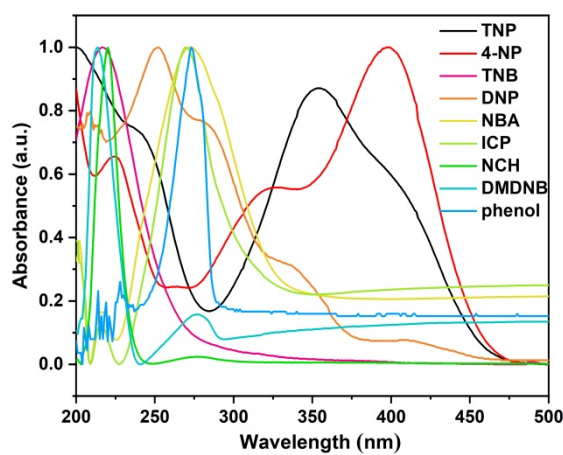


Figure S15 UV-Vis absorption spectra of various nitroaromatics.

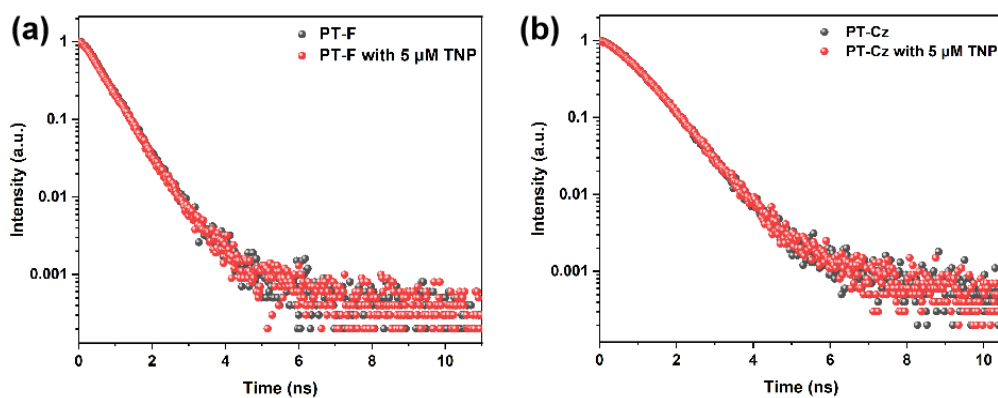


Figure S16 Time resolved fluorescence spectra of (a) PT-F and (c) PT-Cz before and after the addition of TNP.